Received: 16 September 2025 | Accepted: 2 July 2026

DOI: 10.1111/1365-2745.70418

Journal of Ecology

RESEARCH ARTICLE

Climatic niche position predicts population dynamics in Mediterranean shrubs after drought

Teresa Sánchez-Mejía[1,2] | Maria Paniw[3] | Francisco Lloret[1,2]

[1]Universitat Autònoma de Barcelona (UAB), Cerdanyola del Vallès, Spain

[2]Centre de Recerca Ecologica i Aplicacions Forestals (CREAF), Cerdanyola del Vallès, Spain

[3]Estación Biológica de Doñana, Centro Superior de Investigaciones Científicas (EBD-CSIC), Seville, Spain

Correspondence
Teresa Sánchez-Mejía
Email: mariateresa.sanchezme@autonoma.cat

Funding information
Agència de Gestió d'Ajuts Universitaris i de Recerca, Grant/Award Number: 2021 SGR 00849; Ministerio de Ciencia, Tecnología e Innovación, Grant/Award Number: PID2020-115264RB-I00, PID2022-141004OA-I00 and PRE2021-099957; Severo Ochoa Centre of Excellence, Grant/Award Number: CEX2018-000828-S

Handling Editor: Yoann Le Bagousse-Pinguet

Abstract

1. Climate change is altering plant population dynamics by increasing drought frequency and intensity in many regions. The climatic niche (i.e. the range of climatic conditions under which a species persists) offers a powerful framework to link the effects of climate on population performance with species-specific tolerances. However, how the population's position within its species' climatic niche influences population fitness remains poorly understood.
2. We investigated demographic responses to climatic niche position in two Mediterranean shrubs, *Halimium halimifolium* and *Lavandula stoechas*, following an extreme drought in Doñana National Park (SW Spain). Using individual demographic data from 2019 to 2022, we modelled survival, growth and reproduction as functions of distance to each species' climatic niche centroid and of drought-induced vegetation die-off. We then integrated these vital rates into integral projection models (IPMs) to assess population growth.
3. We found that proximity to the niche centroid increased population growth, especially for *H. halimifolium*. In contrast, *L. stoechas* exhibited a more complex pattern, with population growth peaking near the niche centroid but remaining high farther away. These patterns were driven mainly by increased recruitment near the niche centroid, together with reduced seedling survival, suggesting demographic compensation. In both species, small shifts in niche position within the observed range led to substantial demographic changes.
4. Importantly, vegetation die-off further modulated demographic responses to niche position. Population growth in *H. halimifolium* was highest at moderate die-off, likely balancing facilitation and competition. In contrast, *L. stoechas* reached its highest population growth under high die-off, possibly due to competitive release.
5. Perturbation analysis pointed out that changes in population growth in *L. stoechas* were driven mainly by the influence of niche position on early life-stage processes, especially recruitment and seedling survival, whereas in *H. halimifolium* they were mainly influenced by adult survival and growth responses to niche position.
6. *Synthesis*. Our results show that population fitness is shaped by climatic niche position, with higher fitness generally closer to their niche centroid. Niche metrics

This is an open access article under the terms of the Creative Commons Attribution License, which permits use, distribution and reproduction in any medium, provided the original work is properly cited.
© 2026 The Author(s). *Journal of Ecology* published by John Wiley & Sons Ltd on behalf of British Ecological Society.

capture species-specific climatic tolerances and requirements; by incorporating them into demographic models, we can better assess population responses to climatic variability across species and ecosystems.

KEYWORDS
centroid distance, ecological niche, integral projection model, niche centroid, plant demography, population dynamics, vegetation die-off, vital rates

1 | INTRODUCTION

Increasing climatic variability and frequency of extreme climatic events are driving widespread changes in population dynamics and community structure across ecosystems (Allen et al., 2010; Easterling, Meehl, et al., 2000; Hartmann et al., 2022). Among these disturbances, drought has emerged as a major driver of recent vegetation die-off worldwide (Allen et al., 2010; Martínez-Vilalta et al., 2012). In Mediterranean shrublands, drought-induced vegetation die-off has been shown to alter local conditions by disrupting species interactions and modifying resource availability and microclimate (Lloret et al., 2016). Increasing climatic variability can affect species demography by impacting vital rates such as survival (Camarero et al., 2020; Jacobsen & Pratt, 2018), growth (Gazol et al., 2017; Liu et al., 2020) and reproduction (Chamorro et al., 2016; del Cacho et al., 2013). These changes may compromise population viability and ultimately scale up to drive shifts in community structure and ecosystem function (Ma et al., 2015). As climate change is projected to further increase the intensity and frequency of climatic extreme events, particularly in the Mediterranean region (IPCC, 2023), understanding their effects on population dynamics is crucial for maintaining species and community resilience.

Climatic fluctuations may impact vital rates and life stages in different magnitudes and directions (Doak & Morris, 2010; Tenhumberg et al., 2018). These effects may trigger cascading effects on population dynamics if climate influences vital rates in the same direction (Compagnoni et al., 2016; Iler et al., 2019). Conversely, compensatory effects may emerge if climate impacts on vital rates in opposing directions, potentially stabilizing population responses (Knops et al., 2007; Lloret et al., 2012; Ozgul et al., 2023). Nevertheless, such cascading or compensatory effects may diminish or disappear as climatic drivers intensify over time (Conquet et al., 2025; Doak & Morris, 2010). Therefore, methodologies that integrate climate effects across all life cycle stages are essential to assess climate impacts on population persistence fully.

Structured demographic models (e.g. matrix or integral projection models) integrate species' vital rates and provide a robust framework for assessing population dynamics. They have been widely employed to examine the effects of abiotic and biotic drivers (Christiansen et al., 2024; Dahlgren et al., 2016; Paniw et al., 2017, 2023; Stears et al., 2025). Accounting for climatic drivers in these models has advanced our understanding of population responses to climatic variability and helped to identify climatic thresholds for population viability (Adler et al., 2012; Compagnoni et al., 2021; Paniw et al., 2023). However, identifying which climatic variables best explain vital rates and population dynamics is not straightforward. The choice of a climatic predictor strongly influences the detection of links between climate and population dynamics (Evers et al., 2021; Tenhumberg et al., 2018). An additional challenge is that the same climatic conditions may not have the same implication for different species even when they coexist, since their impact depends on how closely those conditions align with each species' climatic optimum or tolerance limits (Carscadden et al., 2020).

Niche theory defines the ecological niche as a multidimensional environmental space in which a species can persist over time (Holt, 2009; Hutchinson, 1978; Pulliam, 2000). Therefore, plant responses to environmental conditions can be interpreted in relation to their location in ecological niches (Perez-Navarro et al., 2022). Specifically, the realized climatic niche (climatic niche, hereafter) is defined by the subset of climatic conditions under which a species is found to live. The climatic niche framework offers a solid theoretical background and an operational approach for integrating species-specific climatic tolerances into demographic analyses. Accordingly, populations closer to the centre of their climatic niche, thus experiencing conditions closer to the species' climatic optimum, would exhibit a better demographic performance, which would decrease towards the niche margins (Brown, 1984; Hengeveld & Haeck, 1982).

Climatic niche metrics are typically linked to vital rates or abundance via climatic suitability indices derived from ecological niche models (ENM) or spatial distribution models (SDM). However, empirical support for this relationship has often been inconsistent (Baer & Maron, 2020; Csergő et al., 2017; Dallas et al., 2017). In contrast, recent studies suggest that niche distances, such as proximity of a population to the climatic niche centroid (i.e. climatic optimum), may better capture demographic responses, especially under conditions of high climatic variability (Perez-Navarro et al., 2022; Ureta et al., 2018). Unlike suitability indices, which assign zero values when conditions fall outside a species' tolerance thresholds, niche distances provide continuous values even for populations occasionally experiencing conditions outside the predicted niche (Broennimann et al., 2021; Perez-Navarro et al., 2022). This makes them especially valuable for studying population persistence under extreme climatic conditions, such as drought events (Perez-Navarro et al., 2022).

In this study, we use integral projection models (IPMs) to assess the role of the species' climatic niche position in shaping the

13652745, 2026, 8, Downloaded from https://besjournals.onlinelibrary.wiley.com/doi/10.1111/1365-2745.70418. By Universitaet Autonoma De, Wiley Online Library on [04/11/2026]. See the Terms and Conditions (https://onlinelibrary.wiley.com/terms-and-conditions) on Wiley Online Library for rules of use; OA articles are governed by the applicable Creative Commons License

demographic responses and resulting population dynamics in a shrubland affected by drought. The study was conducted in Doñana National Park (SW Spain), which experienced an extreme drought event in 2005 followed by persistent but fluctuating drought conditions in the following years. We focused on two common Mediterranean shrub species with contrasting life histories, the long-lived *Halimium halimifolium* and the short-lived *Lavandula stoechas*. Previous research in this area has documented the drought's impact on early recruitment (del Cacho & Lloret, 2012; Lloret et al., 2016) and on community resilience (Paniw et al., 2021). However, the consequences of drought-induced changes in vegetation structure on integrated demographic responses have not been addressed. For instance, the balance between facilitation and competition, which determines recruitment beneath vegetation canopy, may be altered by drought-induced canopy die-off (Díaz-Borrego et al., 2024). Since this system is characterized by high climatic variability and recurrent droughts, it provides a valuable opportunity to assess how climatic niche position interacts with persistent drought effects in shaping demographic responses.

Using individual repeated censuses from 2019 to 2022, we parameterized vital rates as a function of the population's distance to its species' climatic niche centroid and the vegetation die-off (i.e. post-drought vegetation structure). These functions were used to build IPMs and estimate population growth as a proxy for population fitness. We expected population growth to be highest when populations experienced climatic conditions closer to their species' climatic niche centroid driven by higher survival and reproduction. Additionally, we expected that vegetation die-off after drought would modulate this response by altering plant interactions. To assess the influence of niche position and vegetation die-off on population growth, we first simulated population growth across different combinations of observed values for species niche position and vegetation die-off. We also performed a perturbation analysis (i.e. by modifying position in the species niche and die-off in vital rates) to identify through vital rates variation of climate and die-off affected population growth most strongly.

2 | MATERIALS AND METHODS

2.1 | Study system

We conducted the study in Doñana National Park (SW Spain (37°01′ N, 6°32′ W)), in a Mediterranean shrubland known as 'monte blanco', located on stabilized dunes. The study area is dominated by the shrub species *Halimium halimifolium* and *Rosmarinus officinalis*, alongside other halophilic and xerophilic species such as *Halimium commutatum*, *Cistus libanotis*, *Lavandula stoechas*, *Erica scoparia*, *Staurancanthus genistoides*, *Ulex australis*, *Thymus mastichina* and *Helichrysum picardii* (García Murillo & Sousa Martín, 1999).

The climate is Mediterranean with oceanic influence. Based on records from the Doñana Biological Station from 1980 to 2023 (ICT, 2023), the mean annual temperature is 17.3°C, ranging from 10.2°C in January (coldest month) to 24.7°C in August (warmest month). The mean annual rainfall is 504 mm, with interannual variation between 177 mm in dry years to 1186 mm in wet years. In 2005, the study area experienced an extreme drought event followed by an unusually cold winter, resulting in a severe shrubland die-off (Díaz-Delgado, 2006). Subsequent research has documented that the drought's effects on vegetation cover and population dynamics persisted over the following years (Paniw et al., 2021).

For our demographic study, we selected two common shrub species in the system with both contrasted life histories and geographic range sizes. *Halimium halimifolium* (L.) Willk (Cistaceae) is a semi-deciduous shrub of 60–120 cm height occurring on sandy substrates in southwestern Europe and northern Morocco. It is a dominant species in the stabilized sand dunes of Doñana National Park (Zunzunegui González et al., 1997). Its vegetative growth is completed in spring when water is available, and flowering takes place in late spring (Herrera, 1986). *Lavandula stoechas* L. (Lamiaceae) is an evergreen shrub reaching 30–100 cm widely distributed across the Mediterranean basin. In the Iberian Peninsula, it is found in the southern and eastern regions in sunny areas from sea level to 1000 m over neutral and acid soils (Herrera, 1997). Growth and flowering occur from February to May (Herrera, 1986). As *H. halimifolium*, *L. stoechas* does not resprout, and reproduction only occurs through seed production (Herrera, 1987).

2.2 | Demographic data

The study system consisted of 18 plots (5 × 5 m) separated by a minimum distance of 50 m, distributed across an area of 10 km^2. All plots were located on sandy soils with flat topography. The plots were established in 2007, 2 years after the 2005 extreme drought and subsequent mortality event (Díaz-Delgado, 2006). We set the plots along a drought impact gradient based on vegetation cover defoliation, ranging from 5% to 80%. We measured drought-induced vegetation die-off (hereafter, die-off) once in 2007 as the percentage of dead cover relative to the total shrub cover (dead and alive) per plot. We estimated shrub cover using a point-intercept method, recording contacts with branches at 0.5 m intervals along ten 5 m transects E-W oriented within each plot. We categorized contacts as living (branches with leaves or green shoots) or dead canopy (recently defoliated branches with undecomposed leaves on the ground, excluding decayed organs). Characterizing drought impact 2 years after the drought event was supported by NDVI data showing no significant recovery on shrub cover between 2005 and 2007 (Lloret et al., 2016), indicating that post-drought regrowth did not substantially affect the assessment. Although some underestimation of die-off due to tissue decay between the drought event and sampling cannot be excluded, this effect is limited because the study focused on woody branches, which persist longer than more labile tissues such as leaves. Furthermore, as all plots were sampled at the same time following the same approach, any bias associated with tissue decay is expected to be consistent across plots and should not

13652745, 2026, 8, Downloaded from https://besjournals.onlinelibrary.wiley.com/doi/10.1111/1365-2745.70418. By Universitaet Autonoma De, Wiley Online Library on [04/11/2026]. See the Terms and Conditions (https://onlinelibrary.wiley.com/terms-and-conditions) on Wiley Online Library for rules of use; OA articles are governed by the applicable Creative Commons License

affect comparative analysis. See Lloret et al. (2016) and de la Riva et al. (2017) for further discussion on the representativeness of the procedure to estimate drought impact.

We began individual demographic censuses in 2019, tagging and tracking plants of *H. halimifolium* and *L. stoechas*. Censuses were conducted annually each spring (May), coinciding with the flowering season. For each tagged adult plant (>1 year-old), we recorded survival and flowering status (flowering vs. non-flowering), mean height and canopy width (cm), and we visually determined the percentage of green cover. Plant size was calculated as the log-transformed product of height, width and green cover. In each plot, we also recorded the number of newly emerged seedlings of both species. Seedlings were marked but not individually tagged to avoid handling damage; therefore, we assessed seedling survival at the plot level. We classified individuals as seedlings from their first census after emergence until the following census, and those surviving to the next census were classified as saplings. Saplings were individually tagged and incorporated into the individual adult monitoring. From 2019 to 2022, we monitored a total of 454 *H. halimifolium* and 1377 *L. stoechas* individuals.

No specific permits were required to conduct this fieldwork.

2.3 | Climatic niche metrics

To account for changes in the population's position within its species' climatic niches throughout the study period, we used the distance to the climatic niche centroid. To do so, we first built species' climatic niches from the climatic conditions across their geographical distribution.

We obtained occurrence records from the Global Biodiversity Information Facility (GBIF, <www.gbif.org>) and filtered them to avoid taxonomic, geographic and sampling inconsistencies. Specifically, we excluded occurrences not corresponding to the accepted species name (i.e. wrong or inaccurate synonyms), from ex-situ records (i.e. specimens or material) and not georeferenced. We also excluded occurrences collected before 1950 and with high spatial uncertainty (i.e. coordinate uncertainty greater than 1 km) to match the spatial resolution of the climatic dataset (see below). We then extracted climatic data for the filtered occurrences from Easyclimate, a European database that provides daily climatic data at 1 km resolution, using the 'easyclimate' R package (Cruz-Alonso et al., 2023). We aggregated the daily climatic data to monthly minimum and maximum temperature and precipitation, and derived bioclimatic variables using the 'dismo' R package (Hijmans et al., 2023). To reduce spatial autocorrelation and sampling bias, we randomly thinned occurrence records by retaining a single occurrence within the radius defined by the minimum distance at which the relationship between geographic distance and climatic variables was not significantly correlated. We determined this distance using Mantel correlograms implemented in the 'ecospat' R package (Broennimann et al., 2023). When this distance was smaller than the resolution of the Easyclimate dataset (~1 km), we applied a minimum threshold of 1 km to keep consistency between occurrences and climatic data. After filtering, we retained a total of 561 unique occurrence records for *H. halimifolium* and 6124 for *L. stoechas*.

We built a common climatic space for the two species by performing Principal Component Analysis (PCA) on the selected bioclimatic variables. From the 19 bioclimatic variables calculated (Appendix S1, Table S2), we excluded those derived from multiple bioclimatic variables and from the combination of temperature and precipitation as they may complicate the interpretation of PCA axes (Perez-Navarro et al., 2022). Hence, we retained 12 bioclimatic variables: annual mean temperature (bio 1), temperature seasonality (bio 4), maximum temperature of the warmest month (bio 5), minimum temperature of the coldest month (bio6), mean temperature of warmest quarter (bio 10), mean temperature of coldest quarter (bio11), annual precipitation (bio 12), precipitation of the wettest month (bio 13), precipitation of the driest month (bio 14), precipitation seasonality (bio 15), precipitation of wettest quarter (bio 16) and precipitation of driest quarter (bio 17). We then performed a PCA to reduce the 12 bioclimatic variables into a two-dimensional common climatic space (Broennimann et al., 2012). We used yearly values of the variables from 1980 to 2022 across all species occurrence sites. The first two PCA axes explained 71.04% of the climatic variability (Appendix S1, Figure S2).

We characterized species niches within the common climatic space by projecting species' geographical occurrences. We then applied a Gaussian kernel density function from the 'ks' R package (Duong, 2025) with optimal bandwidth determined by cross-validation (Duong & Hazelton, 2005) to smooth the density of occurrences (Broennimann et al., 2012). This produced an occurrence density value for each cell of the climatic space, representing the area of the species' realized niche. To avoid the influence of outliers, we excluded densities below the 0.05 percentile (Broennimann et al., 2012). We then calculated the niche centroid as the gravity centre of the density distribution and defined the niche edge as its perimeter.

We projected the climatic conditions of the 18 plots included in the study into the species' climatic niches by calculating their PCA scores using climatic data from 2019 to 2022 (Figure 1). Then, we estimated climatic niche metrics based on the relative position of each plot within its species' climatic niche. Among the metrics considered (see Appendix S2, Table S3 for a comparison among the climatic niche metrics), we selected the relative centroid distance (RCD), which accounted for the distance to the niche centroid considering the niche breadth. We calculated RCD in each census interval as the Euclidean distance from the population's climatic conditions to the niche centroid divided by the distance to the closest niche edge, following Perez-Navarro et al. (2022). This metric accounts for irregular niche shape and for differences in niche breadth across species. Given the limited spatial extent of the study area (~10 km^2), plots within the same census interval shared near-identical RCD values, such that variation in RCD occurred primarily across census intervals rather than among plots.

13652745, 2026, 8, Downloaded from https://besjournals.onlinelibrary.wiley.com/doi/10.1111/1365-2745.70418. By Universitaet Autonoma De, Wiley Online Library on [04/11/2026]. See the Terms and Conditions (https://onlinelibrary.wiley.com/terms-and-conditions) on Wiley Online Library for rules of use; OA articles are governed by the applicable Creative Commons License

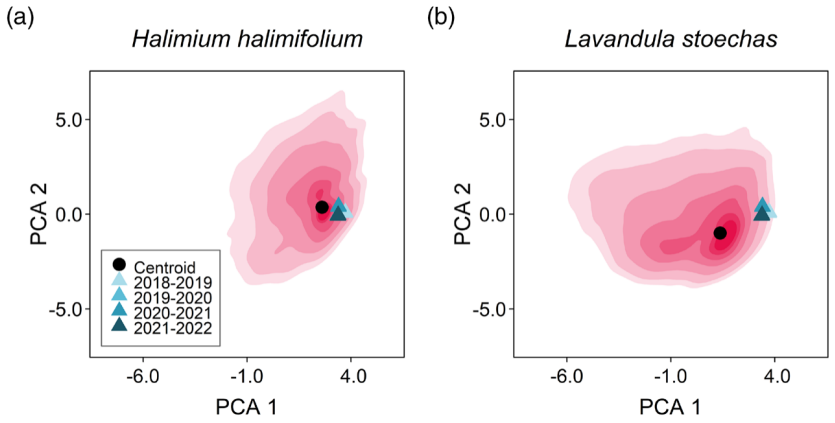


FIGURE 1 Climatic niches of *Halimium halimifolium* (a) and *Lavandula stoechas* (b) projected in the common climatic space defined by the two PCA axes. The climatic niche (pink gradient) was defined from kernel density estimates of species occurrences, with the centroid (black circle) defined as the center of gravity of density values above the 95th percentile. The climatic conditions of the 18 plots surveyed from 2019 to 2022 (blue triangles) are shown within each species' climatic niche. Note that the triangles of 2019–2020 and 2021–2022 overlap due to nearly identical climatic conditions.

2.4 | Vital rate models

We applied General Additive Models (GAMs) to evaluate the effects of the climatic niche position and vegetation die-off on the vital rates driving population dynamics for each studied species. We used GAMs to capture non-linear relationships between predictors and response variables.

We estimated survival separately for the adults (>1 year-old) and the seedlings due to differences in data sampling. Adult survival was modelled at the individual level as a binary variable (alive or dead) from time t to $t+1$. Seedling survival was modelled at the plot level as the proportion of seedlings surviving from time t to $t+1$. We fitted survival models with a logit-link function since the response variable followed a binomial distribution. In the seedling survival model, we included as a weight the number of newly emerged seedlings at time t to account for differences in sample size, giving more weight to survival proportions calculated from a larger number of seedlings.

We defined growth as the individual size at time $t+1$ and sapling size as the size distribution of saplings incorporated into the continuous stage (>1 year-old) between time t to $t+1$. We modelled growth and sapling size with identity-link functions because their response variables followed a normal distribution.

We modelled flowering probability, defined as the presence or absence of inflorescences or flowers at time t, using a logit-link function. We modelled recruitment, estimated as the number of newly emerged seedlings at time $t+1$, with a negative binomial error structure and a log-link function to handle overdispersion. To make the recruitment model more biologically realistic, we included the number of reproductive individuals at time t as an offset. For this purpose, we classified individuals as reproductive or non-reproductive based on their size at first reproduction, using size thresholds obtained from Paniw et al. (2021).

We included relative distance to the climatic niche centroid (RCD), vegetation die-off and their interaction as predictors in the baseline structure of all models. To account for the time frame in which RCD most strongly influenced demographic responses, in *H. halimifolium*, RCD was included at time $t-1$ for adult survival, flowering and sapling size, and at time t for growth, recruitment and seedling survival. In *L. stoechas*, RCD was included at time $t-1$ for flowering and sapling size, and at time t for adult survival, growth, recruitment and seedling survival (see Appendix S2 for details). We modelled adult survival, flowering and growth (size-dependent vital rates) as a function of plant size at time t and all possible two-way interactions with RCD and vegetation die-off. Plot was included as a random effect in these models, but it was excluded from size-independent vital rates (recruitment, seedling survival and sapling size) due to limited sample size (see Appendix S2 for details).

We parameterized GAMs with fixed effects as smooth terms using cubic regression splines (cr). We applied the *s*() function for main effects and the *ti*() function for two-way interactions, setting three knots per covariate ($k=3$). We modelled random effects using the *re*() function. To avoid overfitting, we set the gamma parameter to 1.4. We implemented all models in R version 4.5.1. using the 'mgcv' package (Wood, 2025).

2.5 | Integral projection models

To assess population dynamics, we parameterized integral projection models (IPMs) for each species incorporating climatic niche position and vegetation die-off. IPMs predict population dynamics over discrete time steps using a kernel function that integrates vital rates over a continuous state variable (Easterling, Ellner, & Dixon, 2000). The kernel function was derived from the parameters of the vital rate models described above (Appendix S2, Table S4), with individual size as the continuous state variable. For each species, we built IPMs describing the dynamics of two stages, a discrete stage S representing newly emerged seedlings, and a continuous stage $n(z)$ of >1 year-old individuals, where z

13652745, 2026, 8, Downloaded from https://besjournals.onlinelibrary.wiley.com/doi/10.1111/1365-2745.70418. By Universitaet Autonoma De, Wiley Online Library on [04/11/2026]. See the Terms and Conditions (https://onlinelibrary.wiley.com/terms-and-conditions) on Wiley Online Library for rules of use; OA articles are governed by the applicable Creative Commons License

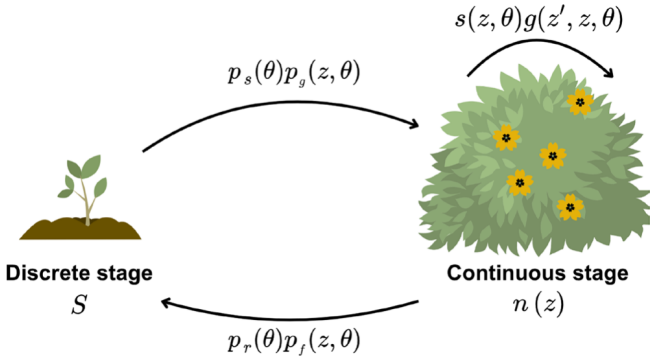


FIGURE 2 Life cycle diagram for *Halimium halimifolium* and *Lavandula stoechas*. The IPM (Equations 1–2) separates the population into a continuous stage $n(z)$ representing >1 year-old individuals and a discrete stage S representing newly emerged seedlings. Seedlings emerge according to flowering probability (p_f) and recruitment (p_r), then either die or transition into the continuous stage. Individuals in the continuous stage, survive (s) and grow (g). Seedling survival (p_s) and sapling size (p_g) determine transitions from the discrete to the continuous stage. Size is represented as z, and the effects of RCD and die-off are represented by θ.

represents individual size (Figure 2). We defined the kernel function as follows:

$$S_{t+1} = p_r(\theta) \int_L^U p_f(z,\theta)\, n_t(z) dz \quad (1)$$

$$n_{t+1}(z') = p_s(\theta) p_g(z,\theta) S_t \int_L^U s(z,\theta) g(z',z,\theta)\; n_t(z) dz \quad (2)$$

The emergence of new seedlings (Figure 2, Equation 1) was modelled as the product of the flowering probability (p_f) of continuous stage individuals of size z and the size-independent probability of seedling recruitment (p_r). After each time step, seedlings either die or transition into the continuous stage. The dynamics of the continuous stage (Figure 2, Equation 2) depend on individuals from both the discrete and continuous stages. Seedlings transitioning to the continuous stage at size z are modelled as the probability of seedling survival (p_s) multiplied by the size distribution of saplings (p_g). Individuals remaining within this stage are described by the survival (s) and growth (g) probabilities as they transition from size z to size z'. The effects of RCD and die-off (θ) were incorporated on population dynamics through the vital rates. For each species, we set the upper (U) and lower (L) limits of the size distribution, to 1.1 times the maximum observed size and L at 0.9 times the minimum observed size, respectively, extending slightly beyond the observed range (Rees et al., 2014). Additionally, to avoid unintentional eviction, individuals with sizes beyond the upper limit U were reassigned to the largest size class (Williams et al., 2012).

IPMs were implemented in R using the midpoint rule (Ellner & Rees, 2006) to discretize the continuous kernel into n-size classes. We selected $n = 100$, resulting in a projection matrix with dimensions $100+1$ by $100+1$, including the discrete seedling stage. Population growth rate (λ) was calculated as the dominant eigenvalue of the matrix. Uncertainty in population projections was addressed using stratified bootstrapping. We performed 100 iterations to resample raw data within each species, census interval and plot. For each resampled dataset, we fitted vital rates and used these parameters to project the population over time (Appendix S3, Figure S4).

2.6 | Effects of climatic niche position and vegetation die-off on population growth rate

To investigate how the population growth rate (λ) varied across the observed gradients of climatic niche position and vegetation die-off, we built separate integral projection models (IPMs) using all possible combinations of the minimum, mean and maximum observed values of relative centroid distance (RCD) and die-off. We addressed uncertainty in λ response across the environmental gradients using bootstrapping, as we explained above.

We also identified which vital rates primarily contributed to changes in λ in response to variation in RCD and die-off using perturbation analyses (Paniw et al., 2023). Specifically, we first built IPMs using full factorial combinations of 750 RCD and 750 die-off values evenly distributed across the observed range. From these models, we randomly selected 300 IPMs with near-stable dynamics ($\lambda \approx 1$, i.e. $0.995 \leq \lambda \leq 1.005$) and retained their corresponding RCD and die-off values combinations. Second, for each of these combinations we built new IPMs increasing either RCD or die-off by 10%. We perturbed each variable (RCD or die-off, respectively) in one vital rate at a time, while the remaining vital rates retained the unperturbed values. Finally, we calculated the percent change in λ under perturbations of RCD or die-off in each vital rate relative to the unperturbed λ rates. Because a 10% increase in RCD or die-off could exceed the observed range for baseline values close to the upper boundary, some perturbations may have involved extrapolation beyond observed conditions. To assess whether such extrapolation affected the interpretation of our analysis, we compared these results with those from an equivalent analysis in which perturbed values were constrained to the corresponding observed maxima, thereby avoiding extrapolation. Both analyses showed that changes in λ in response to perturbation of RCD and die-off occurred through the same vital rates in both species, indicating that the potential inclusion of extrapolated values did not alter the main conclusions. To facilitate interpretation, we retained the full perturbation analysis because it applied a consistent proportional change across baseline combinations of RCD and die-off (see Appendix S4 for details).

3 | RESULTS

3.1 | Effects of climatic niche position and die-off on vital rates

Vital rate responses to centroid distance (RCD) and vegetation die-off differed markedly between the two species, both in shape and strength. Vital rates of *H. halimifolium* were generally higher closer

13652745, 2026, 8, Downloaded from https://besjournals.onlinelibrary.wiley.com/doi/10.1111/1365-2745.70418. By Universitaet Autonoma De, Wiley Online Library on [04/11/2026]. See the Terms and Conditions (https://onlinelibrary.wiley.com/terms-and-conditions) on Wiley Online Library for rules of use; OA articles are governed by the applicable Creative Commons License

Journal of Ecology

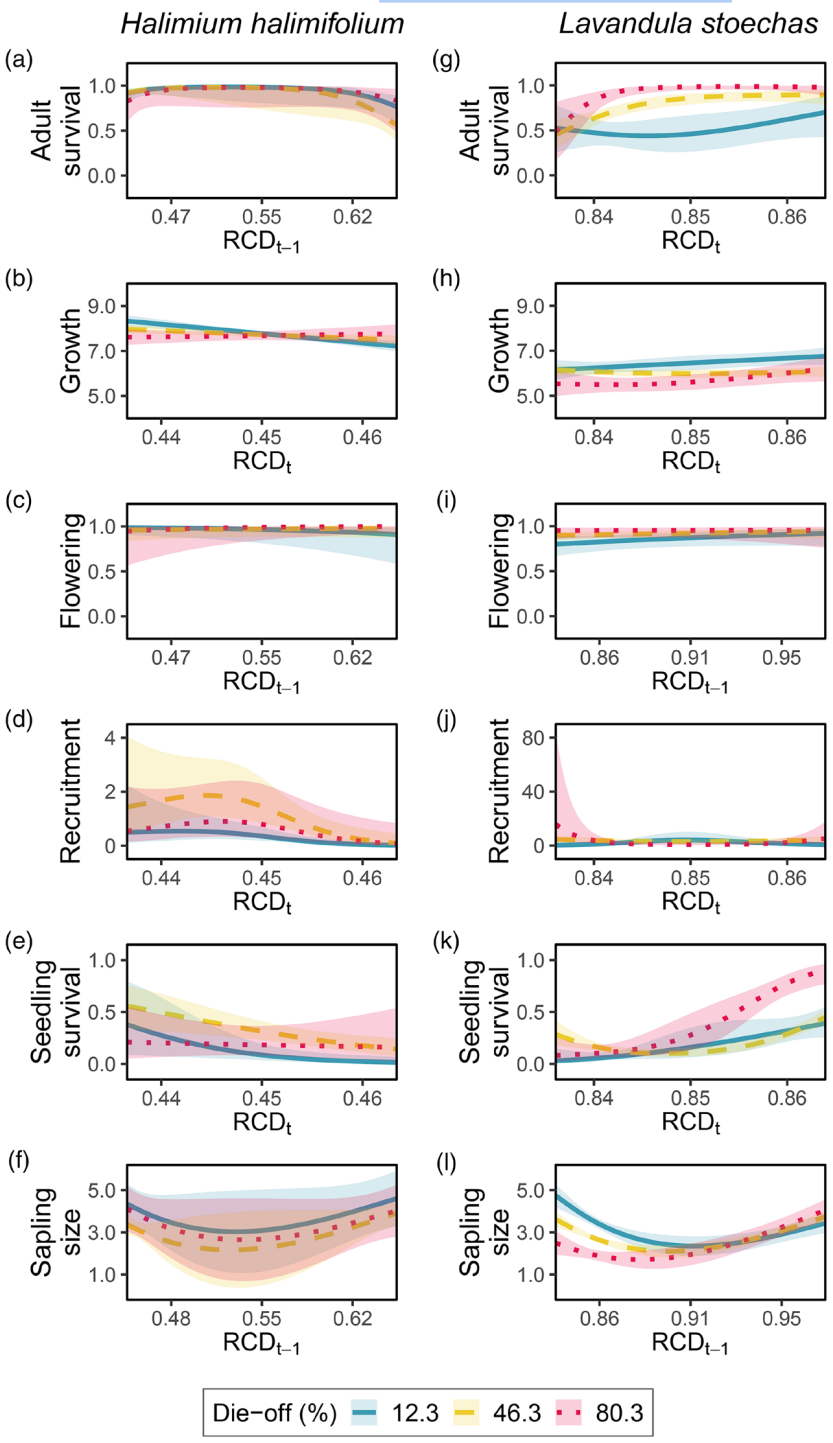


FIGURE 3 Effect of relative distance to the climatic niche centroid (RCD) and vegetation die-off on vital rates of *Halimium halimifolium* and *Lavandula stoechas*. Vital rates (rows) included: adult survival (a, g), growth (b, h), flowering (c, i), recruitment (d, j), seedling survival (e, k) and sapling size (f, l). Predictions (lines) were obtained from GAMs along with their 95% confidence intervals (ribbons). For visualization, we plotted the minimum, mean and maximum vegetation die-off values common to both species. Subscripts of RCD indicate the time frame used for the analysis (t or $t-1$). Random effects were excluded, so predictions represent averages across plots. For size-dependent vital rates, size was set to its mean value.

to the climatic niche centroid, with some peaking at moderate die-off (Figure 3). In contrast, *L. stoechas* showed more complex and variable responses across vital rates; although generally, greatest performance was reached at higher die-off. In addition, *L. stoechas* showed relatively more variable vital rate responses to both gradients (Figure 3).

In *H. halimifolium*, adult survival remained consistently high closer to the niche centroid with little variation across die-off levels (Figure 3a). However, it declined at greater centroid distances, particularly under moderate die-off. Growth declined slightly with increasing centroid distance, also showing little variation across die-off values (Figure 3b). Flowering probability was largely unaffected by either variable (Figure 3c). Recruitment and seedling survival peaked closer to the niche centroid and under moderate die-off (Figure 3d,e). At maximum distance from the centroid, both seedling survival and recruitment were consistently low. Sapling size showed a non-monotonic response, with lower values at intermediate centroid distance and little variation across die-off levels although values were slightly higher under low die-off (Figure 3f).

In *L. stoechas*, adult survival was lowest at minimum centroid distance increasing as niche centroid increases, but this differed across die-off levels (Figure 3g). Under higher die-off, adult survival

13652745, 2026, 8, Downloaded from https://besjournals.onlinelibrary.wiley.com/doi/10.1111/1365-2745.70418. By Universitaet Autonoma De, Wiley Online Library on [04/11/2026]. See the Terms and Conditions (https://onlinelibrary.wiley.com/terms-and-conditions) on Wiley Online Library for rules of use; OA articles are governed by the applicable Creative Commons License

increased sharply still near the niche centroid and stabilized close to 1; whereas under low die-off it increased more gradually, reaching similar values at maximum centroid distance. Growth also increased with increasing centroid distance and was slightly higher under low die-off (Figure 3h). Flowering remained largely constant across centroid distance and die-off levels (Figure 3i). Recruitment showed a high variability and a complex response across the centroid distance and die-off gradients. (Figure 3j). Under high die-off, recruitment peaked near the centroid and then declined at intermediate centroid distance, but under low die-off increased at moderate centroid distance. Seedling survival peaked farther from the niche centroid, particularly under high die-off, while near the centroid it was higher under intermediate die-off (Figure 3k). Sapling size decreased at intermediate centroid distances (Figure 3l), with higher values under low die-off near the niche centroid and little variation across die-off levels farther from the niche centroid.

3.2 | Effects of climatic niche position and die-off on population growth

Population growth rate (λ) was highest closer to the climatic niche centroid in both species, but the strength of this response and its interaction with vegetation die-off differed notably between them (Figure 4). In *H. halimifolium*, λ peaked near the niche centroid (Figure 4a). At intermediate levels of both centroid distance and die-off, λ remained high, but distinctly diminished with both low and high levels of die-off. At further distances from the centroid, λ dropped sharply at intermediate die-off levels. Consequently, population growth was lowest at the greatest centroid distance, with values slightly below 1 irrespective of vegetation die-off. In *L. stoechas*, λ also reached its highest values near the niche centroid under moderate and high die-off, but unlike *H. halimifolium*, λ diminished below 1 when die-off was the lowest (Figure 4b). This pattern changed at intermediate distance from the niche centroid, where λ dropped at higher vegetation die-off, reaching values close to 1, while increasing under low vegetation die-off. At further centroid distance, λ reached intermediate values around 2 across all values of vegetation die-off.

3.3 | Contributions to population growth of vital rate-specific perturbations of climatic niche position and die-off

Variation in population growth (λ) under perturbations of climatic niche centroid distance (RCD) was driven by different vital rates in the two studied species, with adult survival and growth contributing more in *H. halimifolium*, and recruitment and seedling survival in *L. stoechas* (Figure 5). Overall, λ in both species was relatively more responsive to perturbations in specific vital rates of centroid distance than of vegetation die-off.

In *H. halimifolium*, λ responded most strongly to niche position through growth and adult survival (Figure 5a). Increasing centroid distance reduced λ via growth but increased it through adult survival. Perturbations of centroid distance in recruitment, seedling survival and sapling size had smaller effects on λ, decreasing it, while perturbations in flowering had the weakest impact. By contrast, perturbations of die-off in vital rates led to smaller changes in λ, with slightly stronger effects on λ through seedling survival and recruitment.

In *L. stoechas*, changes in λ under perturbations of niche position were mainly driven by the effects of centroid distance in seedling survival and recruitment (Figure 5b). Perturbations of centroid distance in adult survival, growth, flowering and sapling size had much smaller effects on λ. Overall, increasing centroid distance in most vital rates increased λ, except in flowering and sapling size where λ decreased. Changes in λ under perturbations of die-off occurred mainly through seedling survival and recruitment, both increasing λ. Perturbations of die-off in other vital rates had minimal effects on λ.

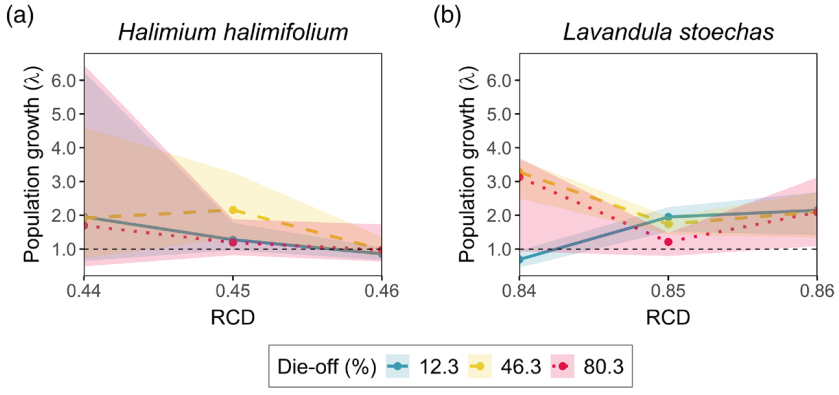


FIGURE 4 Effect of relative distance to the climatic niche centroid (RCD) and vegetation die-off on population growth rates (λ) for *Halimium halimifolium* (a) and *Lavandula stoechas* (b). In each panel, lines represent average population size, and shaded areas indicate 95% bootstrap confidence intervals based on 100 model iterations. The stable population growth rate ($\lambda = 1$) is shown as a dashed horizontal black line. We built integral projection models (IPMs) using the minimum, mean and maximum vegetation die-off values common to both species, and the minimum, mean and maximum RCD values specific to each species.

13652745, 2026, 8, Downloaded from https://besjournals.onlinelibrary.wiley.com/doi/10.1111/1365-2745.70418. By Universitaet Autonoma De, Wiley Online Library on [04/11/2026]. See the Terms and Conditions (https://onlinelibrary.wiley.com/terms-and-conditions) on Wiley Online Library for rules of use; OA articles are governed by the applicable Creative Commons License

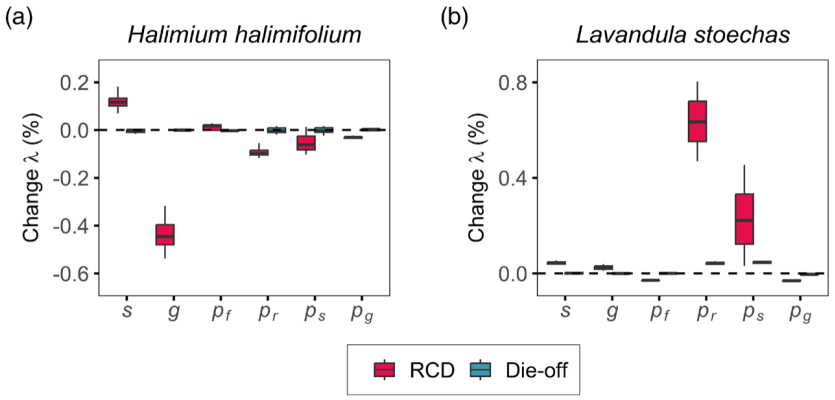


FIGURE 5 Percentage change in population growth rate (λ) at equilibrium ($\lambda \approx 1$) in response to perturbations of 10% increase in relative distance to the climatic niche centroid (RCD) (left boxes) or in vegetation die-off (right boxes), applied separately to each vital rate for *Halimium halimifolium* (a) and *Lavandula stoechas* (b). Vital rates are represented on the *x* axis: adult survival (s), growth (g), flowering probability (p_f), recruitment (p_r), seedling survival (p_s) and sapling size (p_g). Estimates are derived from 300 integral projection models (IPMs) simulations under near-equilibrium conditions.

4 | DISCUSSION

Our study provides evidence that plant vital rates and population growth (λ) may vary strongly along the position of a population within their species-specific climatic niche. Within the climatic gradient captured in our study, we found that overall λ peaked when populations were closer to the species' climatic niche centroid, consistent with ecological niche theory predicting higher fitness closer to optimal climatic conditions (Pulliam, 2000). This pattern aligns with previous studies reporting declines in abundance (Martínez-Meyer et al., 2013; Osorio-Olvera et al., 2020), vital rates (Csergő et al., 2017; Perez-Navarro et al., 2022) and growth rate (Baer & Maron, 2020; Ureta et al., 2018), as conditions deviated from the species' climatic niche optimum. Nonetheless, the strength and shape of these responses differed between species and were further influenced by the interaction with drought-induced vegetation die-off.

Although derived from two Mediterranean shrub species, our findings on the role of climatic niche position in shaping population performance have implications beyond this system. Since climatic niche position expresses the population climatic conditions relative to the species' climatic tolerances (Perez-Navarro et al., 2022), incorporating this information into demographic analysis may improve our ability to capture how climatic variability and extreme events influence population performance across species and ecosystems (Csergő et al., 2017), as documented for desert plants (Ureta et al., 2018) and mountain trees (Lloret & Kitzberger, 2018).

Two main factors may explain the complex population responses to the climatic niche centroid distance we found, particularly in *L. stoechas*. First, the relationship between climatic niche position and some vital rates, especially those associated with early life stages such as recruitment, seedling survival and sapling size, was non-linear. Similar patterns have been reported in other species (Baer & Maron, 2020) and may have strong effects on λ when these vital rates contribute strongly to λ. Such non-linear responses may arise from interactions with local environmental factors such as biotic interactions or microhabitat variability (Baer & Maron, 2020). Second, demographic compensation driven by contrasting stage-specific responses to climate may also contribute to the complex patterns observed. In our study, most vital rates in *H. halimifolium* tended to increase closer to the climatic niche centroid. However, in *L. stoechas*, the responses were more heterogeneous, and notably, while recruitment peaked closer to the niche centroid, other vital rates, such as seedling survival, reached their maximum values farther away. Similar opposing effects among vital rates to climate have been observed in other studies (Iler et al., 2019; Pironon et al., 2018) and may reflect distinct climatic optima across life stages (Pironon et al., 2018; Zurell et al., 2024). For instance, seedlings generally have narrower and distinct tolerance ranges compared to adults (Zurell et al., 2024). These divergent responses may result in demographic compensation, where declines in some vital rates are buffered by increases in others, thereby stabilizing λ across environmental gradients (Doak & Morris, 2010; Lloret et al., 2012; Villellas et al., 2015).

Canopy cover influences demographic responses by modulating microclimatic conditions, resource availability (e.g. light, nutrients, moisture) and biotic interactions such as herbivory, competition and facilitation (Gómez-Aparicio et al., 2005). Consequently, vegetation die-off following a drought event may lead to either beneficial or detrimental effects depending on species' requirements and tolerances and the local conditions (del Cacho & Lloret, 2012; Holmgren et al., 2012). Our findings for *H. halimifolium* showed that λ peaked at intermediate canopy die-off and minimal to intermediate distance to the niche centroid. Perturbation analysis suggested that the response of seedling survival and recruitment to vegetation die-off were likely the main driver of this pattern, as these vital rates contributed most to the projected changes in λ. However, as these results are based on model simulations, they should be interpreted with some caution. One possible explanation is that moderate vegetation die-off may result in a balance between reduced competitive pressure from the established adult vegetation and facilitation through microclimatic

13652745, 2026, 8, Downloaded from https://besjournals.onlinelibrary.wiley.com/doi/10.1111/1365-2745.70418. By Universitaet Autonoma De, Wiley Online Library on [04/11/2026]. See the Terms and Conditions (https://onlinelibrary.wiley.com/terms-and-conditions) on Wiley Online Library for rules of use; OA articles are governed by the applicable Creative Commons License

buffering, thereby enhancing performance under moderate shade (Holmgren et al., 2012). This balance could be particularly beneficial for vulnerable life stages like seedlings, although further studies would be needed to directly evaluate these mechanisms.

However, this demographic benefit of moderate vegetation die-off on *H. halimifolium* λ was not observed under more stressful climatic conditions (i.e. farther from the climatic niche centroid). While seedlings still showed slightly higher survival at intermediate die-off, likely due to some buffering and reduced competition, recruitment remained low across the die-off gradient. In contrast, adult survival declined most at moderate die-off, suggesting that under higher climatic stress, later life stages may experience increased competition and insufficient facilitation under these conditions. Consequently, farther from the niche centroid, λ dropped to values around 1, regardless of vegetation structure. This indicates that for *H. halimifolium*, under harsher conditions, the effects of neighbour interactions and microclimate buffering become minimal, likely because demographic responses are already strongly limited (Csergő et al., 2017).

In contrast, when climatic conditions were closer to the niche centroid, *L. stoechas* λ was highest at high canopy die-off and lowest at low canopy die-off. This suggests that under more favourable climatic conditions, competitive release and regeneration opportunities due to canopy loss may outweigh the negative effects of losing microclimatic buffering (Lloret et al., 2016). Consistent with this, previous studies have reported increased reproductive output in *L. stoechas* following canopy removal (Herrera, 1997). Still, recruitment under strong die-off was highly variable, suggesting the influence of additional factors such as microsite conditions, seed availability or stochasticity (Long et al., 2014). However, farther from the niche centroid, λ responses in *L. stoechas* were similar across vegetation die-off levels. This shows that the strong effect of vegetation die-off observed under more favourable climatic conditions, likely associated with competence, diminishes under harsher climates. Such a shift is consistent with previous evidence that plant interactions generally change with increasing environmental stress, often due to reduced competition (He et al., 2013).

While survival and recruitment were influenced by climatic niche position and canopy die-off in both species, growth and especially flowering showed weaker responses. The limited response of flowering may partially reflect methodological limitations of using binary flowering presence as a proxy for reproductive performance. Future studies should consider additional reproductive metrics (e.g. flower number, seeds per flower and seed germination success) to characterize more accurately reproductive performance.

Despite these weaker effects, both growth and flowering still contributed to variation in λ when climatic niche position and die-off were perturbed. In *H. halimifolium* responses of λ to variation in climatic niche position were driven primarily through growth and adult survival. In contrast, in *L. stoechas*, niche position influenced λ mainly via early life-stage processes, especially recruitment and seedling survival, while adult survival and growth showed minimal contributions to the response of λ to niche position. These distinct responses likely reflect differences in life-history strategies between the relatively short-lived *L. stoechas* and the longer-lived *H. halimifolium*. In long-lived species with slow life histories, λ is typically more sensitive to survival-growth than to fecundity (Moutouama & Gaoue, 2023) and is generally buffered against environmental variability (Morris et al., 2008; Paniw et al., 2018). Conversely, short-lived species with fast life histories depend more on reproduction, making them more sensitive to environmental variability (Morris et al., 2008; Paniw et al., 2018; Postuma et al., 2020). This difference may explain the greater demographic variability observed in *L. stoechas* in response to changes in niche position and vegetation die-off.

More broadly, these differences in how vital rates responded to climatic niche position and contributed to λ indicate that climatic effects on population dynamics may be misrepresented when inferred from a single vital rate. Integrating responses across the full life cycle is therefore necessary to assess the overall consequences of climatic niche position for population viability (Doak & Morris, 2010; Villellas et al., 2015) and to compare climate effects among species, where the vital rates driving population dynamics may differ (Morris et al., 2008; Paniw et al., 2018).

Several demographic responses to niche position and die-off were non-linear, suggesting potential ecological thresholds where small shifts in environmental conditions could trigger abrupt population declines (Baer & Maron, 2020; Chevalier et al., 2021). Although demographic compensation can buffer populations against environmental variation (Doak & Morris, 2010; Villellas et al., 2015), this buffering may weaken near the edges of species' climatic tolerance (Doak & Morris, 2010). Temporary displacements from the niche centroid may have limited effects if followed by favourable conditions, depending on their duration and magnitude (Perez-Navarro et al., 2022), while sustained deviations from optimal conditions could gradually undermine population viability (Doak & Morris, 2010; Morris et al., 2008). Here, we focused on the short-term demographic responses to shifts in climatic conditions, rather than on the cumulative impacts that may arise over time, and we found that, even small shifts in climatic niche position led to substantial changes in population responses.

Nonetheless, some limitations of our study should be considered when interpreting our results. Because the study area covered a relatively small spatial extent, variation in the distance to the climatic niche centroid occurred primarily among census intervals and only minimally among plots. Consequently, the effective replication of climatic conditions in our study was limited, increasing the risk of pseudoreplication and reducing the strength of inference regarding climatic effects (Hurlbert, 1984). This temporal structure also limited our ability to separate the effects of climatic niche position on vital rates from other unmeasured year-specific conditions, such as biotic interactions or other environmental variation. In this regard, the interaction between climatic niche position and vegetation die-off should be interpreted with some caution, as part of the observed responses may reflect temporal variation beyond differences directly associated with climatic niche position. Therefore, increasing climatic replication through longer temporal series and wider spatial

13652745, 2026, 8, Downloaded from https://besjournals.onlinelibrary.wiley.com/doi/10.1111/1365-2745.70418. By Universitaet Autonoma De, Wiley Online Library on [04/11/2026]. See the Terms and Conditions (https://onlinelibrary.wiley.com/terms-and-conditions) on Wiley Online Library for rules of use; OA articles are governed by the applicable Creative Commons License

extent will be important to strengthen statistical inference and disentangle niche position effects from other year-specific processes. This would also enable evaluation of population responses across a broader range of climatic conditions.

In addition, our analyses relied on gridded macroclimatic data at 1km spatial resolution, which captures regional climatic conditions rather than the fine-scale microclimate experienced by individual plants. Local and micro-local temperature and moisture can deviate substantially from macroclimatic conditions due to canopy structure, topography, soil properties and water balance (De Frenne et al., 2021). Recent evidence suggests that demographic responses can be better explained by microclimatic than macroclimatic conditions (Christiansen et al., 2024). Studies analysing population responses to climatic niche position may thus benefit from incorporating microclimate data to better capture biologically relevant climatic conditions.

Finally, while we explicitly analysed how the persistent effects of drought-induced vegetation die-off modulated demographic responses to climatic niche position, other ecological drivers may also interact with climatic niche position to influence population performance (Ickin et al., 2025). Incorporating drivers, such as density dependence, biotic interactions and microhabitat heterogeneity, may further improve our understanding of population dynamics along the climatic niche.

5 | CONCLUSIONS

The effects of climatic variability on plant populations can only be fully understood in relation to their species-specific tolerances. The climatic niche captures these tolerances and helps assess whether populations are operating near optimal conditions or approaching their climatic limits. Within the climatic conditions examined here, we found that small shifts in niche position were associated with substantial changes in vital rates and population growth, highlighting the importance of climatic niche position as a driver of population performance.

The effects of climatic niche position, however, were not uniform across vital rates or species and were further modulated by drought-induced vegetation die-off, showing the relevance of accounting for the full life cycle and relevant ecological drivers when evaluating climatic effects on population dynamics.

Overall, our findings suggest that combining climatic niche metrics with structured demographic models provides a useful framework for assessing species-specific responses to climatic variability. In the context of ongoing climatic change, such approaches may help identify populations exposed to less favourable climatic conditions and assess how climatic variability may compromise population viability across species and ecosystems.

AUTHOR CONTRIBUTIONS

Teresa Sánchez-Mejía, Maria Paniw and Francisco Lloret conceived the ideas and designed methodology; Teresa Sánchez-Mejía, Maria Paniw and Francisco Lloret collected the data; Teresa Sánchez-Mejía and Maria Paniw analysed the data; Teresa Sánchez-Mejía led the writing of the manuscript. All authors contributed critically to the drafts and gave final approval for publication.

ACKNOWLEDGEMENTS

TSM received a predoctoral fellowship (PRE2021-099957) funded by MCIN/AEI/10.13039/501100011033 and the European Social Fund (ESF+), within the Severo Ochoa Centre of Excellence grant (CEX2018-000828-S). This work was supported by the funding of the Spanish Ministry of Science and Innovation through the RESIBIO project (PID2020-115264RB-I00) and the Government of Catalonia through AGAUR grant (2021 SGR 00849). MP was funded by MCIN/AEI/10.13039/501100011033 and by the 'ERDF A way of making Europe' project PID2022-141004OA-I00. We thank Hanna Serediuk, Anaïs Naulleau, Raquel Díaz-Borrego, Nuria J. Elvira, Luciana Jaime and María Ángeles Pérez-Navarro for their contribution to the field surveys, and Raquel Díaz-Borrego and María Ángeles Pérez-Navarro for their advice in building species' climatic niches.

CONFLICT OF INTEREST STATEMENT

The authors declare no conflicts of interest.

PEER REVIEW

The peer review history for this article is available at https://www.webofscience.com/api/gateway/wos/peer-review/10.1111/1365-2745.70418.

DATA AVAILABILITY STATEMENT

Occurrences of *Halimium halimifolium* and *Lavandula stoechas* were obtained from the Global Biodiversity Information Facility (GBIF; http://www.gbif.org). Climatic data used to build the climatic niche models and calculate climatic niche metrics were obtained from the Easyclimate dataset (https://github.com/VeruGHub/easyclimate), while climatic data describing the average climatic conditions of the study site were obtained from the ICTS-RBD (https://meteorologia-palacio.icts-donana.es/). Data and code used for demographic analysis are available at https://github.com/MTSM05/ShrubsRBD_ClimaticNicheIPM. A permanent version has been archived in Zenodo and is available at https://doi.org/10.5281/zenodo.21336515 (Sánchez-Mejía et al., 2026).

STATEMENT ON INCLUSION

Our work was conducted by scientists based in the country where the study took place. The perspective of locally based authors who have strong experience with the focal system was paramount to ensure our conclusions reflected the local context. All authors were engaged from the outset in study design, data analysis and interpretation. Additionally, we relied on literature previously published by scientists from the region, and efforts were made to consider relevant work published in the local language.

ORCID

Teresa Sánchez-Mejía https://orcid.org/0000-0001-9745-273X
Francisco Lloret https://orcid.org/0000-0002-9836-4069

13652745, 2026, 8, Downloaded from https://besjournals.onlinelibrary.wiley.com/doi/10.1111/1365-2745.70418. By Universitaet Autonoma De, Wiley Online Library on [04/11/2026]. See the Terms and Conditions (https://onlinelibrary.wiley.com/terms-and-conditions) on Wiley Online Library for rules of use; OA articles are governed by the applicable Creative Commons License

REFERENCES

Adler, P. B., Dalgleish, H. J., & Ellner, S. P. (2012). Forecasting plant community impacts of climate variability and change: When do competitive interactions matter? *Journal of Ecology*, *100*(2), 478–487. https://doi.org/10.1111/j.1365-2745.2011.01930.x

Allen, C. D., Macalady, A. K., Chenchouni, H., Bachelet, D., McDowell, N., Vennetier, M., Kitzberger, T., Rigling, A., Breshears, D. D., Hogg, E. H. (Ted), Gonzalez, P., Fensham, R., Zhang, Z., Castro, J., Demidova, N., Lim, J. H., Allard, G., Running, S. W., Semerci, A., & Cobb, N. (2010). A global overview of drought and heat-induced tree mortality reveals emerging climate change risks for forests. *Forest Ecology and Management*, *259*(4), 660–684. https://doi.org/10.1016/j.foreco.2009.09.001

Baer, K. C., & Maron, J. L. (2020). Ecological niche models display nonlinear relationships with abundance and demographic performance across the latitudinal distribution of *Astragalus utahensis* (Fabaceae). *Ecology and Evolution*, *10*(15), 8251–8264. https://doi.org/10.1002/ece3.6532

Broennimann, O., Di Cola, V., & Guisan, A. (2023). ecospat: Spatial ecology miscellaneous methods. R package version 3.5.1. https://CRAN.R-project.org/package=ecospat

Broennimann, O., Fitzpatrick, M. C., Pearman, P. B., Petitpierre, B., Pellissier, L., Yoccoz, N. G., Thuiller, W., Fortin, M.-J., Randin, C., Zimmermann, N. E., Graham, C. H., & Guisan, A. (2012). Measuring ecological niche overlap from occurrence and spatial environmental data. *Global Ecology and Biogeography*, *21*(4), 481–497. https://doi.org/10.1111/j.1466-8238.2011.00698.x

Broennimann, O., Petitpierre, B., Chevalier, M., González-Suárez, M., Jeschke, J. M., Rolland, J., Gray, S. M., Bacher, S., & Guisan, A. (2021). Distance to native climatic niche margins explains establishment success of alien mammals. *Nature Communications*, *12*(1), 2353. https://doi.org/10.1038/s41467-021-22693-0

Brown, J. H. (1984). On the relationship between abundance and distribution of species. *The American Naturalist*, *124*(2), 255–279. https://doi.org/10.1086/284267

Camarero, J. J., Gazol, A., Sánchez-Salguero, R., Sangüesa-Barreda, G., Díaz-Delgado, R., & Casals, P. (2020). Dieback and mortality of junipers caused by drought: Dissimilar growth and wood isotope patterns preceding shrub death. *Agricultural and Forest Meteorology*, *291*, 108078. https://doi.org/10.1016/j.agrformet.2020.108078

Carscadden, K. A., Emery, N. C., Arnillas, C. A., Cadotte, M. W., Afkhami, M. E., Gravel, D., Livingstone, S. W., & Wiens, J. J. (2020). Niche breadth: Causes and consequences for ecology, evolution, and conservation. *The Quarterly Review of Biology*, *95*(3), 179–214. https://doi.org/10.1086/710388

Chamorro, D., Parra, A., & Moreno, J. M. (2016). Reproductive output, seed anatomy and germination under water stress in the seeder *Cistus ladanifer* subjected to experimental drought. *Environmental and Experimental Botany*, *123*, 59–67. https://doi.org/10.1016/j.envexpbot.2015.11.002

Chevalier, M., Broennimann, O., & Guisan, A. (2021). Using a robust multi-settings inference framework on published datasets still reveals limited support for the abundant centre hypothesis: More testing needed on other datasets. *Global Ecology and Biogeography*, *30*(11), 2211–2228. https://doi.org/10.1111/geb.13376

Christiansen, D. M., Römer, G., Dahlgren, J. P., Borg, M., Jones, O. R., Merinero, S., Hylander, K., & Ehrlén, J. (2024). High-resolution data are necessary to understand the effects of climate on plant population dynamics of a forest herb. *Ecology*, *105*(1), e4191. https://doi.org/10.1002/ecy.4191

Compagnoni, A., Bibian, A. J., Ochocki, B. M., Rogers, H. S., Schultz, E. L., Sneck, M. E., Elderd, B. D., Iler, A. M., Inouye, D. W., Jacquemyn, H., & Miller, T. E. X. (2016). The effect of demographic correlations on the stochastic population dynamics of perennial plants. *Ecological Monographs*, *86*(4), 480–494. https://doi.org/10.1002/ecm.1228

Compagnoni, A., Pardini, E., & Knight, T. M. (2021). Increasing temperature threatens an already endangered coastal dune plant. *Ecosphere*, *12*(3), 03454. https://doi.org/10.1002/ecs2.3454

Conquet, E., Ozgul, A., Gómez-González, S., Ojeda, F., & Paniw, M. (2025). Climate change is associated with a higher extinction risk of a subshrub in anthropogenic landscapes. *Journal of Ecology*, *113*(11), 3124–3140. https://doi.org/10.1111/1365-2745.70150

Cruz-Alonso, V., Pucher, C., Ratcliffe, S., Ruiz-Benito, P., Astigarraga, J., Neumann, M., Hasenauer, H., & Rodríguez-Sánchez, F. (2023). The easyclimate R package: Easy access to high-resolution daily climate data for Europe. *Environmental Modelling and Software*, *161*, 105627. https://doi.org/10.1016/j.envsoft.2023.105627

Csergő, A. M., Salguero-Gómez, R., Broennimann, O., Coutts, S. R., Guisan, A., Angert, A. L., Welk, E., Stott, I., Enquist, B. J., McGill, B., Svenning, J. C., Violle, C., & Buckley, Y. M. (2017). Less favourable climates constrain demographic strategies in plants. *Ecology Letters*, *20*(8), 969–980. https://doi.org/10.1111/ele.12794

Dahlgren, J. P., Bengtsson, K., & Ehrlén, J. (2016). The demography of climate-driven and density-regulated population dynamics in a perennial plant. *Ecology*, *97*(4), 899–907. https://doi.org/10.1890/15-0804.1

Dallas, T., Decker, R. R., & Hastings, A. (2017). Species are not most abundant in the centre of their geographic range or climatic niche. *Ecology Letters*, *20*(12), 1526–1533. https://doi.org/10.1111/ele.12860

De Frenne, P., Lenoir, J., Luoto, M., Scheffers, B. R., Zellweger, F., Aalto, J., Ashcroft, M. B., Christiansen, D. M., Decocq, G., De Pauw, K., Govaert, S., Greiser, C., Gril, E., Hampe, A., Jucker, T., Klinges, D. H., Koelemeijer, I. A., Lembrechts, J. J., Marrec, R., … Hylander, K. (2021). Forest microclimates and climate change: Importance, drivers and future research agenda. *Global Change Biology*, *27*(11), 2279–2297. https://doi.org/10.1111/gcb.15569

de la Riva, E. G., Lloret, F., Pérez-Ramos, I. M., Marañón, T., Saura-Mas, S., Díaz-Delgado, R., & Villar, R. (2017). The importance of functional diversity in the stability of Mediterranean shrubland communities after the impact of extreme climatic events. *Journal of Plant Ecology*, *10*(2), 281–293. https://doi.org/10.1093/jpe/rtw027

del Cacho, M., & Lloret, F. (2012). Resilience of Mediterranean shrubland to a severe drought episode: The role of seed bank and seedling emergence. *Plant Biology*, *14*(3), 458–466. https://doi.org/10.1111/j.1438-8677.2011.00523.x

del Cacho, M., Peñuelas, J., & Lloret, F. (2013). Reproductive output in Mediterranean shrubs under climate change experimentally induced by drought and warming. *Perspectives in Plant Ecology, Evolution and Systematics*, *15*(6), 319–327. https://doi.org/10.1016/j.ppees.2013.07.001

Díaz-Borrego, R., Pérez-Navarro, M. Á., Jaime, L., Elvira, N. J., & Lloret, F. (2024). Climatic disequilibrium of recruit communities across a drought induced die-off gradient in Mediterranean shrubland. *Oikos*, *2024*(7), e10465. https://doi.org/10.1111/oik.10465

Díaz-Delgado, R. (2006). *Evento de mortalidad en la vegetación terrestre del Parque Nacional de Doñana*. Estación Biológica de Doñana, CSIC.

Doak, D. F., & Morris, W. F. (2010). Demographic compensation and tipping points in climate-induced range shifts. *Nature*, *467*(7318), 959–962. https://doi.org/10.1038/nature09439

Duong, T. (2025). ks: Kernel Smoothing. R package version 1.15.1. https://doi.org/10.32614/CRAN.package.ks

Duong, T., & Hazelton, M. L. (2005). Cross-validation bandwidth matrices for multivariate kernel density estimation. *Scandinavian Journal of Statistics*, *32*(3), 485–506. https://doi.org/10.1111/j.1467-9469.2005.00445.x

Easterling, D. R., Meehl, G. A., Parmesan, C., Changnon, S. A., Karl, T. R., & Mearns, L. O. (2000). Climate extremes: Observations, modeling, and impacts. *Science*, *289*(5487), 2068–2074. https://doi.org/10.1126/science.289.5487.2068

Easterling, M. R., Ellner, S. P., & Dixon, P. M. (2000). Size-specific sensitivity: Applying a new structured population model. *Ecology*, *81*(3),

13652745, 2026, 8, Downloaded from https://besjournals.onlinelibrary.wiley.com/doi/10.1111/1365-2745.70418. By Universitaet Autonoma De, Wiley Online Library on [04/11/2026]. See the Terms and Conditions (https://onlinelibrary.wiley.com/terms-and-conditions) on Wiley Online Library for rules of use; OA articles are governed by the applicable Creative Commons License

694–708. https://doi.org/10.1890/0012-9658(2000)081[0694:SSSAAN]2.0.CO;2

Ellner, S. P., & Rees, M. (2006). Integral projection models for species with complex demography. *American Naturalist*, *167*(3), 410–428. https://doi.org/10.1086/499438

Evers, S. M., Knight, T. M., Inouye, D. W., Miller, T. E. X., Salguero-Gómez, R., Iler, A. M., & Compagnoni, A. (2021). Lagged and dormant season climate better predict plant vital rates than climate during the growing season. *Global Change Biology*, *27*(9), 1927–1941. https://doi.org/10.1111/gcb.15519

García Murillo, P., & Sousa Martín, A. (1999). El Paisaje Vegetal de la Zona Oeste del Parque Natural de Doñana (Huelva). *Lagascalia*, *21*(1), 111–132.

Gazol, A., Sangüesa-Barreda, G., Granda, E., & Camarero, J. J. (2017). Tracking the impact of drought on functionally different woody plants in a Mediterranean scrubland ecosystem. *Plant Ecology*, *218*(8), 1009–1020. https://doi.org/10.1007/s11258-017-0749-3

Gómez-Aparicio, L., Gómez, J. M., Zamora, R., & Boettinger, J. L. (2005). Canopy vs. soil effects of shrubs facilitating tree seedlings in Mediterranean montane ecosystems. *Journal of Vegetation Science*, *16*(2), 191–198. https://doi.org/10.1111/j.1654-1103.2005.tb02355.x

Hartmann, H., Bastos, A., Das, A. J., Esquivel-Muelbert, A., Hammond, W. M., Martínez-Vilalta, J., Mcdowell, N. G., Powers, J. S., Pugh, T. A. M., Ruthrof, K. X., & Allen, C. D. (2022). Climate change risks to global Forest health: Emergence of unexpected events of elevated tree mortality worldwide. *Annual Review of Plant Biology*, *58*(21), 673–702. https://doi.org/10.1146/annurev-arplant-102820-012804

He, Q., Bertness, M. D., & Altieri, A. H. (2013). Global shifts towards positive species interactions with increasing environmental stress. *Ecology Letters*, *16*(5), 695–706. https://doi.org/10.1111/ele.12080

Hengeveld, R., & Haeck, J. (1982). The distribution of abundance. I. Measurements. *Journal of Biogeography*, *9*(4), 303–316.

Herrera, J. (1986). Flowering and fruiting phenology in the coastal shrublands of Donana, south Spain. *Vegetatio*, *68*, 91–98.

Herrera, J. (1987). Biología reproductiva de algunas especies de matorral de Doñana. *Anales del Jardin Botánico de Madrid*, *44*(2), 483–497.

Herrera, J. (1997). Effects of disturbance on the reproductive potential of *Lavandula stoechas*, a Mediterranean sclerophyllous shrub. *Ecography*, *20*, 88–95.

Hijmans, R. J., Phillips, S., Leathwick, J., & Elith, J. (2023). dismo: Species Distribution Modeling. R package version 1.3–14. https://CRAN.R-project.org/package=dismo

Holmgren, M., Gómez-Aparicio, L., Quero, J. L., & Valladares, F. (2012). Non-linear effects of drought under shade: Reconciling physiological and ecological models in plant communities. *Oecologia*, *169*(2), 293–305. https://doi.org/10.1007/s00442-011-2196-5

Holt, R. D. (2009). Bringing the Hutchinsonian niche into the 21st century: Ecological and evolutionary perspectives. *Proceedings of the National Academy of Sciences of the United States of America*, *106*(supple.2), 19659–19665. https://doi.org/10.1073/pnas.0905137106

Hurlbert, S. H. (1984). Pseudoreplication and the design of ecological field experiments. *Ecological Monographs*, *54*(2), 187–211. https://doi.org/10.2307/1942661

Hutchinson, G. E. (1978). *An introduction to population ecology*. Yale University Press.

Ickin, E., Conquet, E., Abrahms, B., Albon, S. D., Blumstein, D. T., Bond, M. L., Boersma, P. D., Clark-Wolf, T. J., Clutton-Brock, T., Compagnoni, A., Dostálek, T., Evers, S. M., Fichtel, C., Gamelon, M., García-Callejas, D., Griesser, M., Hansen, B. B., Jenouvrier, S., Jerstad, K., … Paniw, M. (2025). Comparative life-cycle analyses reveal interacting climatic and biotic drivers of population responses to climate change. *PNAS Nexus*, *4*(9), pgaf286. https://doi.org/10.1093/pnasnexus/pgaf286

ICTS – Infraestructuras Científicas y Técnicas Singulares. (2023). *ICTS-RBD data series (1980–2022)*. http://icts.ebd.csic.es

Iler, A. M., Compagnoni, A., Inouye, D. W., Williams, J. L., CaraDonna, P. J., Anderson, A., & Miller, T. E. X. (2019). Reproductive losses due to climate change-induced earlier flowering are not the primary threat to plant population viability in a perennial herb. *Journal of Ecology*, *107*(4), 1931–1943. https://doi.org/10.1111/1365-2745.13146

IPCC. (2023). Summary for policymakers. In Core Writing Team, H. Lee, & J. Romero (Eds.), *Climate change 2023: Synthesis report. Contribution of working groups I, II and III to the sixth assessment report of the Intergovernmental Panel on Climate Change* (pp. 1–34). IPCC. https://doi.org/10.59327/IPCC/AR6-9789291691647.001

Jacobsen, A. L., & Pratt, R. B. (2018). Extensive drought-associated plant mortality as an agent of type-conversion in chaparral shrublands. *New Phytologist*, *219*(2), 498–504. https://doi.org/10.1111/nph.15186

Knops, J. M. H., Koenig, W. D., & Carmen, W. J. (2007). Negative correlation does not imply a tradeoff between growth and reproduction in California oaks. *Proceedings of the National Academy of Sciences*, *104*(43), 16982–16985. https://doi.org/10.1073/pnas.0704251104

Liu, D., Zhang, C., Ogaya, R., Estiarte, M., & Peñuelas, J. (2020). Effects of decadal experimental drought and climate extremes on vegetation growth in Mediterranean forests and shrublands. *Journal of Vegetation Science*, *31*(5), 768–779. https://doi.org/10.1111/jvs.12902

Lloret, F., de la Riva, E. G., Pérez-Ramos, I. M., Marañón, T., Saura-Mas, S., Díaz-Delgado, R., & Villar, R. (2016). Climatic events inducing die-off in Mediterranean shrublands: Are species' responses related to their functional traits? *Oecologia*, *180*(4), 961–973. https://doi.org/10.1007/s00442-016-3550-4

Lloret, F., Escudero, A., Iriondo, J. M., Martínez-Vilalta, J., & Valladares, F. (2012). Extreme climatic events and vegetation: The role of stabilizing processes. *Global Change Biology*, *18*(3), 797–805. https://doi.org/10.1111/j.1365-2486.2011.02624.x

Lloret, F., & Kitzberger, T. (2018). Historical and event-based bioclimatic suitability predicts regional forest vulnerability to compound effects of severe drought and bark beetle infestation. *Global Change Biology*, *24*(5), 1952–1964. https://doi.org/10.1111/gcb.14039

Long, Q., Foster, B. L., & Kindscher, K. (2014). Seed and microsite limitations mediate stochastic recruitment in a low-diversity prairie restoration. *Plant Ecology*, *215*(11), 1287–1298. https://doi.org/10.1007/s11258-014-0387-y

Ma, G., Rudolf, V. H. W., & Ma, C. S. (2015). Extreme temperature events alter demographic rates, relative fitness, and community structure. *Global Change Biology*, *21*(5), 1794–1808. https://doi.org/10.1111/gcb.12654

Martínez-Meyer, E., Díaz-Porras, D., Peterson, A. T., & Yáñez-Arenas, C. (2013). Ecological niche structure and rangewide abundance patterns of species. *Biology Letters*, *9*(1), 20120637. https://doi.org/10.1098/rsbl.2012.0637

Martínez-Vilalta, J., Lloret, F., & Breshears, D. D. (2012). Drought-induced forest decline: Causes, scope and implications. *Biology Letters*, *8*(5), 685–691. https://doi.org/10.1098/rsbl.2011.1059

Morris, W. F., Pfister, C. A., Tuliapurkar, S., Haridas, C. V., Boggs, C. L., Boyce, M. S., Bruna, E. M., Church, D. R., Coulson, T., Doak, D. F., Forsyth, S., Gaillard, J.-M., Horvitz, C. C., Kalisz, S., Kendall, B. E., Knight, T. M., Lee, C. T., & Menges, E. S. (2008). Longevity can buffer plant and animal populations against changing climatic variability. *Ecology*, *89*(1), 19–25. https://doi.org/10.1890/07-0774.1

Moutouama, J. K., & Gaoue, O. G. (2023). Effects of range and niche position on the population dynamics of a tropical plant. *Ecology*, *104*(4), e3990. https://doi.org/10.1002/ecy.3990

Osorio-Olvera, L., Yañez-Arenas, C., Martínez-Meyer, E., & Peterson, A. T. (2020). Relationships between population densities and niche-centroid distances in north American birds. *Ecology Letters*, *23*, 555–564. https://doi.org/10.1111/ele.13453

13652745, 2026, 8, Downloaded from https://besjournals.onlinelibrary.wiley.com/doi/10.1111/1365-2745.70418. By Universitaet Autonoma De, Wiley Online Library on [04/11/2026]. See the Terms and Conditions (https://onlinelibrary.wiley.com/terms-and-conditions) on Wiley Online Library for rules of use; OA articles are governed by the applicable Creative Commons License

Ozgul, A., Fichtel, C., Paniw, M., & Kappeler, P. M. (2023). Destabilizing effect of climate change on the persistence of a short-lived primate. *Proceedings of the National Academy of Sciences of the United States of America*, *120*(14), e2214244120. https://doi.org/10.1073/pnas.2214244120

Paniw, M., de la Riva, E. G., & Lloret, F. (2021). Demographic traits improve predictions of spatiotemporal changes in community resilience to drought. *Journal of Ecology*, *109*(9), 3233–3245. https://doi.org/10.1111/1365-2745.13597

Paniw, M., García-Callejas, D., Lloret, F., Bassar, R. D., Travis, J., & Godoy, O. (2023). Pathways to global-change effects on biodiversity: New opportunities for dynamically forecasting demography and species interactions. *Proceedings of the Royal Society B: Biological Sciences*, *290*(1993), 20221494. https://doi.org/10.1098/rspb.2022.1494

Paniw, M., Ozgul, A., & Salguero-Gómez, R. (2018). Interactive life-history traits predict sensitivity of plants and animals to temporal autocorrelation. *Ecology Letters*, *21*(2), 275–286. https://doi.org/10.1111/ele.12892

Paniw, M., Quintana-Ascencio, P. F., Ojeda, F., & Salguero-Gómez, R. (2017). Interacting livestock and fire may both threaten and increase viability of a fire-adapted Mediterranean carnivorous plant. *Journal of Applied Ecology*, *54*(6), 1884–1894. https://doi.org/10.1111/1365-2664.12872

Perez-Navarro, M. A., Broennimann, O., Esteve, M. A., Bagaria, G., Guisan, A., & Lloret, F. (2022). Comparing climatic suitability and niche distances to explain populations responses to extreme climatic events. *Ecography*, *2022*(11), e06263. https://doi.org/10.1111/ecog.06263

Pironon, S., Villellas, J., Thuiller, W., Eckhart, V. M., Geber, M. A., Moeller, D. A., & García, M. B. (2018). The 'Hutchinsonian niche' as an assemblage of demographic niches: Implications for species geographic ranges. *Ecography*, *41*(7), 1103–1113. https://doi.org/10.1111/ecog.03414

Postuma, M., Schmid, M., Guillaume, F., Ozgul, A., & Paniw, M. (2020). The effect of temporal environmental autocorrelation on eco-evolutionary dynamics across life histories. *Ecosphere*, *11*(2), e03029. https://doi.org/10.1002/ecs2.3029

Pulliam, H. R. (2000). On the relationship between niche and distribution. *Ecology Letters*, *3*, 349–361. https://doi.org/10.1046/j.1461-0248.2000.00143.x

Rees, M., Childs, D. Z., & Ellner, S. P. (2014). Building integral projection models: A user's guide. *Journal of Animal Ecology*, *83*(3), 528–545. https://doi.org/10.1111/1365-2656.12178

Sánchez-Mejía, T., Paniw, M., & Lloret, F. (2026). Climatic niche position predicts population dynamics in Mediterranean shrubs after drought (Version v1) [Computer software]. *Zenodo*. https://doi.org/10.5281/zenodo.21336515

Stears, A. E., Heidel, B., Paniw, M., Salguero-Gómez, R., & Laughlin, D. C. (2025). Negative density dependence promotes persistence of a globally rare yet locally abundant plant species (*Oenothera coloradensis*). *Oikos*, *2025*(1), e10673. https://doi.org/10.1111/oik.10673

Tenhumberg, B., Crone, E. E., Ramula, S., & Tyre, A. J. (2018). Time-lagged effects of weather on plant demography: Drought and *Astragalus scaphoides*. *Ecology*, *99*(4), 915–925. https://doi.org/10.1002/ecy.2163

Ureta, C., Martorell, C., Cuervo-Robayo, Á. P., Mandujano, M. C., & Martínez-Meyer, E. (2018). Inferring space from time: On the relationship between demography and environmental suitability in the desert plant *O. rastrera*. *PLoS One*, *13*(8), e0201543. https://doi.org/10.1371/journal.pone.0201543

Villellas, J., Doak, D. F., García, M. B., & Morris, W. F. (2015). Demographic compensation among populations: What is it, how does it arise and what are its implications? *Ecology Letters*, *18*(11), 1139–1152. https://doi.org/10.1111/ele.12505

Williams, J. L., Miller, T. E. X., Ellner, S. P., & Doak, D. F. (2012). Avoiding unintentional eviction from integral projection models. *Ecology*, *93*(9), 2008–2014. https://doi.org/10.1890/11-2147.1

Wood, S. N. (2025). mgcv: Mixed GAM computation vehicle with automatic smoothness estimation. R package version 1.9-4. https://CRAN.R-project.org/package=mgcv

Zunzunegui González, M., Díaz Antunes-Barradas, M. C., & García Novo, F. (1997). Autoecological notes of "Halimium Halimifolium" at Doñana National Park. *Lagascalia*, *19*(1–2), 725–736.

Zurell, D., Zimmermann, N. E., & Brun, P. (2024). The niche through time: Considering phenology and demographic stages in plant distribution models. *Journal of Ecology*, *112*(9), 1926–1939. https://doi.org/10.1111/1365-2745.14361

SUPPORTING INFORMATION

Additional supporting information can be found online in the Supporting Information section at the end of this article.

Appendix S1. Climatic niche characterization.

Table S1. Statistics comparing monthly climatic data from Easyclimate and the Doñana Biological Station (DBS), including Pearson correlation coefficient (*r*), root mean square error (RMSE), mean absolute error (MAE) and bias (DBS—Easyclimate).

Figure S1. Comparison of monthly precipitation, minimum temperature and maximum temperature from Easyclimate and the Doñana Biological Station (DBS). Each grey point represents one monthly observation. The red line shows the least-squares regression fit.

Table S2. Description of bioclimatic variables (BIO) from the 'dismo' R package (Hijmans et al., 2023) and indication of their use for the climate niche modelling of *H. halimifolium* and *L.stoechas*.

Figure S2. Common climatic space within the climatic niches of *Halimium halimifolium* and *Lavandula stoechas*. The correlation circle was obtained from the Principal Component Analysis (PCA) of the 12 selected bioclimatic variables (see Appendix S1, Table S2 for details). PCA was performed using climatic data from 561 and 6124 occurrences of *Halimium halimifolium* and *Lavandula stoechas*, respectively, across their European distribution. The first and second axes of the PCA contained 41.3% and 29.8%, respectively, of the explained variability. The colour of the variable represents its percentage contribution to the PCA. PCA1 corresponds to an aridity gradient, with positive values associated with higher temperatures and precipitation seasonality and negative values to higher precipitation. PCA2 corresponds to a humidity gradient, with positive values associated with higher precipitation and negative values with higher temperature seasonality.

Appendix S2. Model selection of vital rates.

Table S3. Climatic niche variables selection using Akaike criteria (AICc). For each vital rate, models were fitted using the same fixed and random effects except for the climatic variable. Climatic variables included: centroid distance (CD), edge distance (ED), relative centroid distance (RCD) and relative edge distance (RED). Selected models are highlighted in bold.

Table S4. Final vital rate models (GAMs) used for Integral Projection Models (IPMs). RCD (relative centroid distance), Size (plant size at time *t*) and Die-off (vegetation Die-off %). Subscripts indicate time frame (*t* or *t* − 1) of RCD, and asterisk interaction among variables. Dev % (total) indicates the percentage of deviance explained by the final model including both fixed and random effects, while Dev % (fixed) indicates the percentage of deviance explained by a model including only fixed effects.

13652745, 2026, 8, Downloaded from https://besjournals.onlinelibrary.wiley.com/doi/10.1111/1365-2745.70418. By Universitaet Autonoma De, Wiley Online Library on [04/11/2026]. See the Terms and Conditions (https://onlinelibrary.wiley.com/terms-and-conditions) on Wiley Online Library for rules of use; OA articles are governed by the applicable Creative Commons License

Figure S3. Effect of relative distance to the climatic niche centroid (RCD) and vegetation die-off (Die-off %) on vital rates of *Halimium halimifolium* and *Lavandula stoechas*. Vital rates (rows) included: adult survival, growth, flowering, recruitment, seedling survival and sapling size. Predictor variables (RCD and die-off) are displayed in columns. Predictions (lines: orange for size-dependent vital rates, purple for size-independent vital rates) were obtained from GAMs with 95% confidence intervals (ribbons). For size-dependent vital rates, size was fixed at the 25th, 50th and 75th percentiles. In *H. halimifolium*, RCD was included at time $t-1$ for adult survival, flowering and sapling size, and at time t for growth, recruitment and seedling survival, while in *L. stoechas*, RCD was included at time $t-1$ for flowering and sapling size, and at time t for adult survival, growth, recruitment and seedling survival. Fixed effects not displayed were set to their mean values. Random effects were excluded, so predictions represent averages across plots.

Appendix S3. Population size from Integral Projection Model (IPMs) simulations.

Figure S4. Population size of *Halimium halimifolium* (top panel) and *Lavandula stoechas* (bottom panel), comparing observed data with integral projection model (IPM) simulations. Lines represent average population size per plot, while shaded areas indicate 95% bootstrap confidence intervals based on 100 model iterations. Points represent observed population size per plot.

Appendix S4. Evaluation of perturbation analysis.

Figure S5. Percentage change in population growth rate (λ) at equilibrium ($\lambda \approx 1$) in response to 10% perturbation increase in relative distance to the climatic niche centroid (RCD) (left boxes) or in vegetation die-off (right boxes), applied separately to each vital rate for (a) *Halimium halimifolium* and (b) *Lavandula stoechas*. For each species, the left panel shows perturbation analysis using unconstrained perturbation, whereas the right panel shows analyses in which perturbed values were constrained to the maximum observed value of each environmental variable. Vital rates are represented on the x axis: adult survival (s), growth (g), flowering probability (p_f), recruitment (p_r), seedling survival (p_s) and sapling size (p_g). Estimates were obtained from 300 Integral Projection Models (IPMs) simulations under near-equilibrium conditions.

How to cite this article: Sánchez-Mejía, T., Paniw, M., & Lloret, F. (2026). Climatic niche position predicts population dynamics in Mediterranean shrubs after drought. *Journal of Ecology*, *114*, e70418. https://doi.org/10.1111/1365-2745.70418

13652745, 2026, 8, Downloaded from https://besjournals.onlinelibrary.wiley.com/doi/10.1111/1365-2745.70418. By Universitaet Autonoma De, Wiley Online Library on [04/11/2026]. See the Terms and Conditions (https://onlinelibrary.wiley.com/terms-and-conditions) on Wiley Online Library for rules of use; OA articles are governed by the applicable Creative Commons License